Available online at www.sciencedirect.com

ScienceDirect

Procedia Structural Integrity 5 (2017) 817–824

Structural Integrity Procedia

www.elsevier.com/locate/procedia

2nd International Conference on Structural Integrity, ICSI 2017, 4-7 September 2017, Funchal, Madeira, Portugal

Optimal notched specimen parameters for accurate fatigue critical distance determination

C. Santus[a], D. Taylor[b], M. Benedetti[c,*]

[a]*Department of Civil and Industrial Engineering, University of Pisa, Pisa, Italy*
[b]*Department of Mechanical & Manufacturing Engineering, Trinity College Dublin, Dublin, Ireland*
[c]*Department of Industrial Engineering, University of Trento, Trento, Italy*

Abstract

The critical distance value should theoretically be determined from the plain specimen fatigue limit and the threshold stress intensity factor, though usually ordinary notch geometries are considered. In this paper, we proposed an optimized sharp notch with the aims of simple and reliable manufacture and, more importantly, a local strong stress gradient able to minimize the sensitivity on the deduced critical distance value. A numerical procedure is proposed to find the critical distance from the fatigue strength of the notched specimen, by implementing the line method with simple formulas based on dimensionless equations and specific coefficients derived from accurate FE analyses. A definition of the boundaries for a valid critical distance evaluation is also introduced and discussed. Finally, an application example is provided on a quenched and tempered steel also comparing the obtained critical distances with the threshold derived values.

Peer-review under responsibility of the Scientific Committee of ICSI 2017

Keywords: Critical distance determination; Line method; Dimensionless analysis; Inversion problem; Q+T 42CrMo4 steel

1. Introduction

The theory of critical distance is a widespread and reliable tool for assessing the strength of notched components in particular under fatigue loading (Taylor (2007), Taylor (2008)) and recently extended in many fatigue areas such as residual stress effects Benedetti et al. (2010) or even fretting fatigue Bertini and Santus (2015).

* Corresponding author. Tel.: +39-046-1282457
E-mail address: matteo.benedetti@unitn.it

2452-3216
Peer-review under responsibility of the Scientific Committee of ICSI 2017
10.1016/j.prostr.2017.07.057

Nomenclature

ΔK_{th}	Threshold stress intensity factor, full range.
$\Delta\sigma_{fl}$	Plain specimen fatigue limit, full range.
L	Fatigue critical distance.
$\Delta\sigma_y$	Notch axial stress, full range.
$\Delta\sigma_N$	Notched specimen (net) nominal stress, full range.
$\Delta\sigma_{N,fl}$	Notched specimen fatigue limit, nominal stress, full range.
K_f	Fatigue stress concentration factor.
D	Specimen external diameter.
R	Notch radius.
A	Notch depth.
ρ	R/A notch radius ratio.
α	Notch angle.
s	Williams linear elastic power law singularity exponent.
K_N	Notch stress intensity factor.
$K_{N,U}$	Notch stress intensity factor for unitary stress.
$K_{N,UU}$	Notch stress intensity factor for unitary stress and unitary half diameter.
$\Delta\sigma_{av,0}$	Average stress according to the line method, zero radius notch, full range.
$\Delta\sigma_{av}$	Average stress according to the line method, radiused notch, full range.
l_{min}, l_{max}	Minimum and maximum limits for the range of accurate dimensionless critical distance determination.
γ_{min}, γ_{max}	Minimum and maximum limits for the range of the inversion function.

Different methods can be formalized within the theory. Among them, the Line method is the most commonly used, unless multiaxial fatigue is involved where the Point method may be preferential, as proposed by Bagni et al. (2016). On the other hand, Benedetti et al. (2016) recently explored the possibility of combining an area method and the Crossland multiaxial criterion with the aim to eliminate the dependence on the load ratio.

According to the basic definition of the Critical Distance, its determination is obtained by combining the threshold stress intensity factor full range ΔK_{th} and the plain specimen fatigue limit full range $\Delta\sigma_{fl}$:

$$L = \frac{1}{\pi}\left(\frac{\Delta K_{th}}{\Delta\sigma_{fl}}\right)^2 \tag{1}$$

However, an accurate evaluation of the threshold may be a difficult experimental task, thus any sharply notched specimen can be considered as an alternative to the fracture mechanics test to estimate the L value (Taylor (2011)), or even the threshold after the inversion of Eq. 1. This approach has been supported in particular by Susmel and Taylor (2010) also extending this method to the determination of the fracture toughness. In the present paper, the use of a reference sharp notch specimen is deeply investigated, with the aim of defining an optimal geometry, and providing a formulation to straightforwardly calculate the critical distance without the need of a finite element simulation.

2. Notched specimen critical distance inversion

Among the several notched specimen geometries, such as those shown by Hu et al. (2013), the V-shaped notch on a round specimen is here considered, both to avoid the edge effect, which may play a role in a flat specimen, and to easily manufacture the notch detail with a relatively small root radius. Initially, a stress analysis is here reported about the ideal perfectly sharp geometry with the stress singularity, Fig. 1 (a), still useful as a reference, then the radiused notch is approached, Fig. 1 (b).

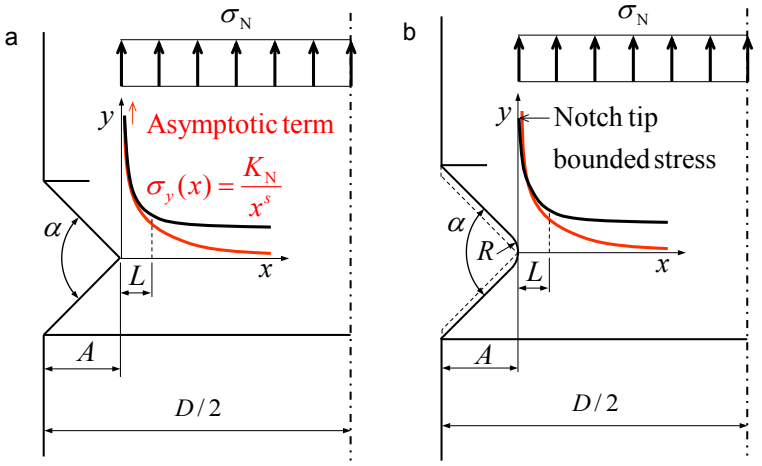

Fig. 1. Local geometry, dimensions and stress distributions for round specimens with V-shaped (a) sharp notch; (b) radiused notch.

2.1. Perfectly sharp notch

The power law singularity exponent, according to the local Williams' solution, depends on the notch angle. This dependence is reported in Fig. 2 (a) along with the values for the two most common angles, in agreement with those available in Atzori et al. (2005) and Hills and Dini (2011).

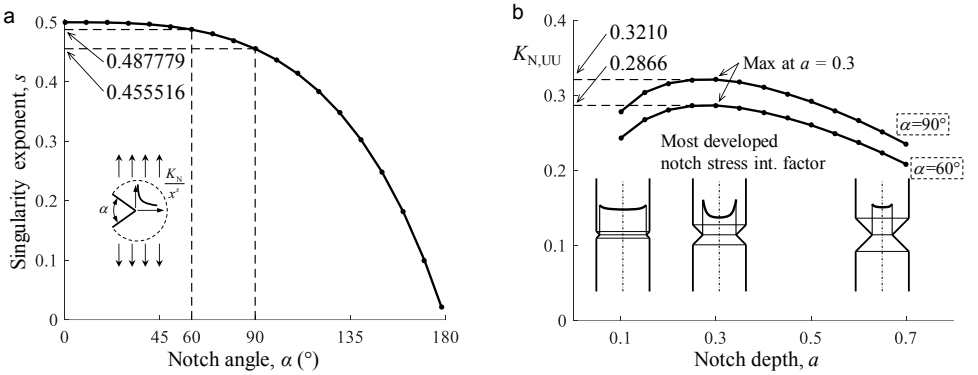

Fig. 2. (a) Williams linear elastic power law singularity exponent, specific values for the notch angles α = 60°, 90°; (b) Unitary notch stress intensity factor dependence on the notch depth.

The singularity term of the local stress distribution is reported below and, owing to the stress linearity, $K_{N,U}$ [mm^s] can be defined as the notch stress intensity factor for unitary nominal stress:

$$\sigma_y(x) = \frac{K_N}{x^s}, \qquad \sigma_y(x) = \sigma_N \frac{K_{N,U}}{x^s} \tag{2}$$

Furthermore, the self-similarity of the solution suggests rescaling the length of the problem. After selecting a reference dimension (D/2 has been considered here, Fig. 1 (a)) a purely dimensionless notch stress intensity factor can be introduced as:

$$\sigma_y(\xi)=\sigma_{\mathrm{N}}\frac{K_{\mathrm{N,UU}}}{\xi^s},\qquad \xi=\frac{x}{D/2},\qquad K_{\mathrm{N,UU}}=K_{\mathrm{N,U}}(D/2)^{-s} \tag{3}$$

$K_{\mathrm{N,UU}}$ is dimensionless, in fact it is the notch stress concentration factor for unitary nominal stress and for unitary scaling length, i.e. when the specimen radius (D/2) equals unity. The value of $K_{\mathrm{N,UU}}$ can be obtained by means of FE simulations (here not reported for brevity) and only depends on the dimensional ratios, and not on the size of the specimen, viz. on the α angle and the relative notch depth $a = A/(D/2)$. The maximum at $a = 0.3$ is evident, Fig. 2 (b). At this intermediate depth, the dimensionless stress intensity factor is highest, providing the strongest gradient dominated region ahead of the notch root. For this reason, this optimal depth is then considered for the following investigated geometry with radiused notch.

The Line Method stress averaging can be put in a dimensionless form too:

$$\frac{1}{2L}\int_0^{2L}\Delta\sigma_y(x)\mathrm{d}x=\frac{1}{2l}\int_0^{2l}\Delta\sigma_y(\xi)\mathrm{d}\xi \tag{4}$$

Where the dimensionless critical distance $l = L/(D/2)$ is here introduced. By considering just the singular term of the stress distribution, the line method integration can be rewritten as:

$$\Delta\sigma_{\mathrm{av},0}(l)=\frac{1}{2l}\int_0^{2L}\Delta\sigma_{\mathrm{N}}\frac{K_{\mathrm{N,UU}}}{\xi^s}\mathrm{d}\xi=\frac{\Delta\sigma_{\mathrm{N}}}{1-s}\frac{K_{\mathrm{N,UU}}}{(2l)^s} \tag{5}$$

in which "0" stands for zero radius notch. According to the line method, this stress has to be equal to the plain specimen fatigue limit, and the estimated (dimensionless) critical distance can be calculated under this hypothesis, and then rearranged according to the K_{f} definition:

$$\Delta\sigma_{\mathrm{fl}}=\frac{\Delta\sigma_{\mathrm{N,fl}}}{1-s}\frac{K_{\mathrm{N,UU}}}{(2l_0)^s},\qquad K_{\mathrm{f}}=\frac{\Delta\sigma_{\mathrm{fl}}}{\Delta\sigma_{\mathrm{N,fl}}},\qquad K_{\mathrm{f}}=\frac{1}{1-s}\frac{K_{\mathrm{N,UU}}}{(2l_0)^s} \tag{6}$$

This latter power equation can be easily reversed, and then the length dimension regained just by multiplying by the reference size D/2. Finally, an easier approximated form is also proposed:

$$l_0=\frac{1}{2}\left(\frac{K_{\mathrm{N,UU}}}{(1-s)K_{\mathrm{f}}}\right)^{1/s},\qquad L_0=\frac{D}{4}\left(\frac{K_{\mathrm{N,UU}}}{(1-s)K_{\mathrm{f}}}\right)^{1/s},\qquad L_{0,\mathrm{aprx}}=D\left(\frac{K_{\mathrm{N,UU}}}{K_{\mathrm{f}}}\right)^{1/s} \tag{7}$$

The equation for L_0 (or alternatively $L_{0,\mathrm{aprx}}$) has a similitude with Eq. 1, though apparently in a different form. Indeed, it offers a direct formula for the critical distance determination, and it is a simple model for the size effect. Obviously, if the α angle were zero, the crack geometry would result, thus $s = 0.5$ and $L_0 = L_{0,\mathrm{aprx}}$. For $\alpha = 60°$ the discrepancy between L_0 and $L_{0,\mathrm{aprx}}$ is approximately 1.5% and it only raises to 5% for $\alpha = 90°$.

2.2. Radiused notch specimen

A certain radius needs to be considered since the ideal perfectly sharp notch is unrealistic, and it is recommended to be accurately controlled. The notch root radius variable R is therefore introduced, Fig. 1 (b), and obviously it is a primary geometry parameter. The dimensionless radius $r = R/(D/2)$ is also defined, according to the previous formulation, and finally a root radius ratio shape parameter is useful to be introduced: $\rho = R/A$ (= r/a). The stress distribution is now bounded with a relatively severe gradient, in which the size of the material critical distance needs to be compared. Two extreme, and not appropriate, conditions can be found:

- The critical distance is very small in comparison to the local radius, Fig. 3 (a), thus the stress gradient is relatively not high within the averaging length.
- The critical distance is too large relatively to the specimens size, thus the integration length is larger than the high gradient region, Fig. 3 (b).

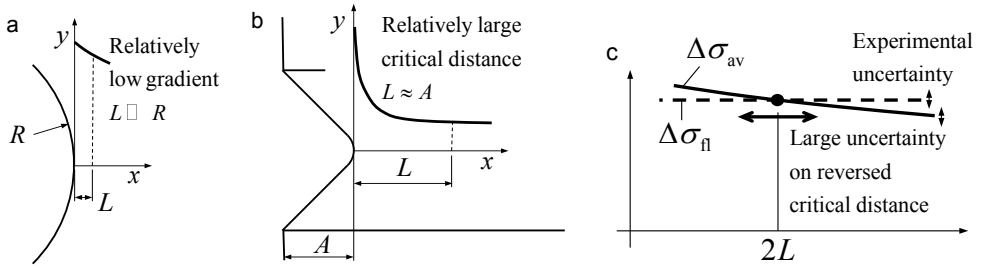

Fig. 3. Extreme cases for the critical distance: (a) very small with respect to the local radius, (b) large with respect to the notch depth; (c) Uncertainty resulting on the evaluation of the critical distance for any low gradient stress distribution.

In both cases, a potential variation of the critical distance implies a small variation of the averaged stress. Conversely, the accuracy of the reverse search is limited, Fig. 3 (c), since any small error, for example due to any experimental issue, implies a significant variation of the predicted critical distance value. In other words, both the notch and the plain specimen tests are low gradient, thus the critical distance is derived from the comparison of two almost parallel lines. On the contrary, in its original definition, the plain specimen should be combined with the long crack which has the highest gradient.

Including the effect of the notch radius, Eq. 5 can be rewritten by introducing a correction function $f(l)$, which for a specific geometry shape only depends on the integration length, i.e. the dimensionless critical distance:

$$\Delta\sigma_{\mathrm{av}}(l) = \Delta\sigma_{\mathrm{N}} \frac{f(l)}{1-s} \frac{K_{\mathrm{N,UU}}}{(2l)^s} \tag{8}$$

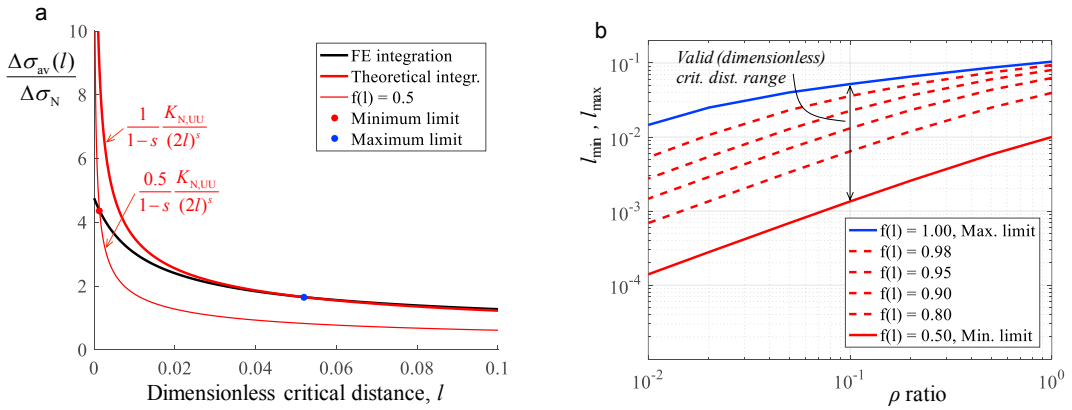

Fig. 4. (a) Dimensionless critical distance limit values for $\rho = 0.1$; (b) Limiting values depending on the radius ratio.

Since the stress distribution is bounded, $f(l)$ tends to zero for small l, thus its discrepancy with the unitary value can be considered to define a useful range for the inversion. The minimum dimensionless critical distance has been set according to a certain fraction, and 0.5 was found to be an effective value, Fig. 4 (a). If the critical distance is smaller

than this reference limit, the notch radius is relatively too high, inducing a low gradient stress in the averaging region. On the other hand, if the critical distance is relatively too large, the stress distribution far from the notch again shows low gradient, as described above. This latter scenario was identified when the numerical integration of the simulated stress distribution overtakes the singularity integration, in other words when $f(l) > 1.0$. Therefore, the range $0.5 \leq f(l) \leq 1.0$ was selected, and then a series of radius ratios ρ was analyzed, Fig. 4 (b).

After introducing the fatigue stress concentration factor K_f in Eq. 8, and the l_0 definition according to Eq. 7, an *inversion function* was defined as: $\gamma(l) = l/f(l)^{1/s}$, and the equation to be inverted reduced to a very simple form:

$$K_f = \frac{f(l)}{1-s}\frac{K_{N,UU}}{(2l)^s}, \qquad \frac{l}{f(l)^{1/s}} = l_0, \qquad \gamma(l) = l_0 \tag{9}$$

In this latter equation the unknown is the (dimensionless) critical distance l, while l_0 can be regarded as an initial tentative value for l.

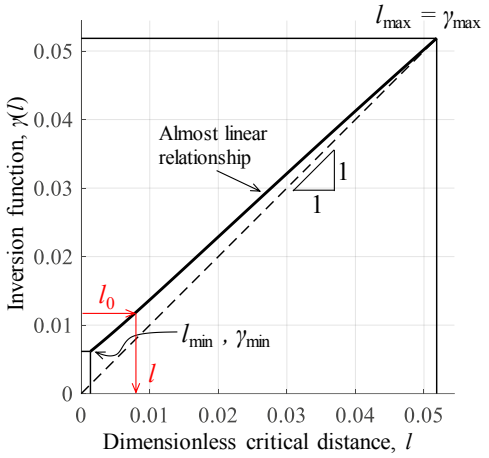

Fig. 5. Almost perfect linearity and boundaries of the inversion function.

The dependence of $\gamma(l)$ turned out to be quite accurately approximated by a linear relationship (see for example Fig. 5 for $\rho = 0.1$). Thus the inversion problem, in dimensionless form, is a simple linear equation:

$$l = l_{min} + \frac{l_{max} - l_{min}}{\gamma_{max} - \gamma_{min}}(l_0 - \gamma_{min}) \tag{10}$$

After having solved Eq. 10, the dimensionless l is easily converted into the L value: $L = D/2\ l$. In order to provide the limits for l and γ, the following fit models have been proposed:

$$\begin{aligned} l_{min} &= p_1\rho^3 + p_2\rho^2 + p_3\rho + p_4 \\ \gamma_{min} &= q_1\rho^3 + q_2\rho^2 + q_3\rho + q_4 \\ l_{max} &= \gamma_{max} = c_1 + c_2\rho^{c_3} \end{aligned} \tag{11}$$

The coefficients of Eq. 11, derived from accurate numerical simulations, are listed in Tab. 1 for a large range of the notch radius ratio ρ and for the two most common V notch angles $\alpha = 90°$ and $60°$. As discussed above, l_{min} and l_{max} are not only the coefficients for Eq. 11, but they also provide the effective range recommended for the critical distance inversion, i.e. to avoid the high sensibility cases of Fig. 3 and equivalently have $0.5 \leq f(l) \leq 1.0$.

Table 1. p_i, q_i, c_i fit coefficients for the γ, l limit values as function of the notch radius ratio ρ.

Notch angle α = 90°, notch depth a = 0.3, notch radius ratio range ρ = 0.01 – 1.0			
$p_1 = 1.5332\times10^{-3}$	$p_2 = -5.4477\times10^{-3}$	$p_3 = 1.3930\times10^{-2}$	$p_4 = 4.3940\times10^{-6}$
$q_1 = 3.0471\times10^{-3}$	$q_2 = -1.8507\times10^{-2}$	$q_3 = 6.1618\times10^{-2}$	$q_4 = -8.6254\times10^{-5}$
$c_1 = -7.8701\times10^{-2}$	$c_2 = 1.8323\times10^{-1}$	$c_3 = 1.4606\times10^{-1}$	
Notch angle α = 60°, notch depth a = 0.3, notch radius ratio range ρ = 0.01 – 1.0			
$p_1 = 3.4760\times10^{-3}$	$p_2 = -1.0042\times10^{-2}$	$p_3 = 1.8483\times10^{-2}$	$p_4 = 1.3622\times10^{-5}$
$q_1 = 1.1537\times10^{-2}$	$q_2 = -3.7191\times10^{-2}$	$q_3 = 7.5317\times10^{-2}$	$q_4 = 1.4765\times10^{-4}$
$c_1 = 1.7720\times10^{-2}$	$c_2 = 8.6435\times10^{-2}$	$c_3 = 3.2025\times10^{-1}$	

3. Experimental validation

An experimental validation is reported in the present paper, and a deeper investigation is undertaken by the authors at the present. The Quenched and Tempered steel 42CrMo4 was fatigue tested with positive near zero load ratio (R=0.1). This steel was preliminarily characterized as tensile test, obtaining QT steel common properties: yield and ultimate strengths 730 MPa and 875 MPa respectively, elongation at break 17.6% and reduction in area 57.7%. Such high strength steel was expected to have large notch sensitivity which in turn implies a quite short critical distance, in the order of a few tens of microns (Taylor (2007)). For this reason, the insert tool nose radius was selected as quite small. On the other hand, a too sharp tip was not to be prescribed either, since the tip self-blunting can happen because of the material high hardness. The chosen radius was R = 0.2 mm, Fig. 6 (a).

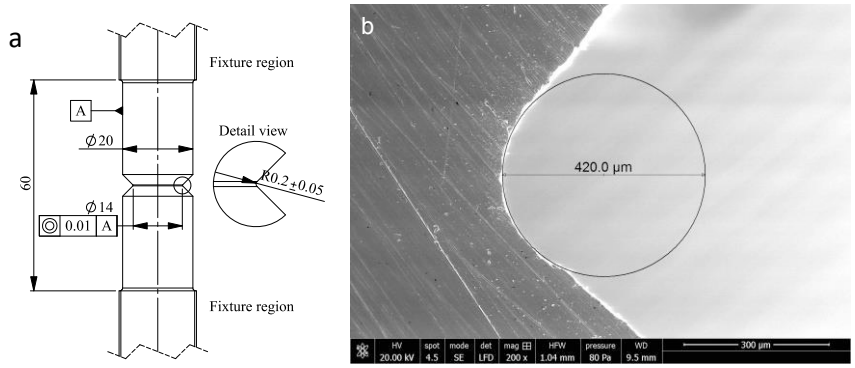

Fig. 6. (a) Notched specimen drawing with the dimensions used in the experimental validation; (b) SEM visualization of the notch root.

According to Eqs. 12 the effective critical distance ranged from 0.0091 mm and 0.447 mm. Since high strength alloys have small value critical distances, the minimum of the range was the most limiting. However, it was successfully verified at the end of the determination procedure. Particular attention was paid to this detail, indeed Fig. 6 (b) shows the SEM assessment of the notch radius, and it was found just slightly larger than the nominal value. Fatigue tests on plain and cylindrical specimens are reported in Fig. 7 (a) and also a threshold test was performed at the same load ratio for a final comparison. Both the C(T) and all the cylindrical specimens have been manufactured from the same batch of round bars, and also the load line was carefully aligned with the axis of the bar to avoid any effect of material inhomogeneity and/or anisotropy. The analytical procedure here introduced gave as result: L = 0.038 mm. This critical distance was then compared with the threshold derived length (Eq. 1), providing the value L = 0.036 mm, which can be considered very well in agreement. This validation was then repeated about the load ratio R=-1. The threshold was found with the M(T) specimen, and the obtained value was L = 0.042 mm to be compared to the proposed procedure result L = 0.031 mm obtained with the same notched specimen. This latter comparison can still be considered satisfactory though the slight opposite trend with respect to R.

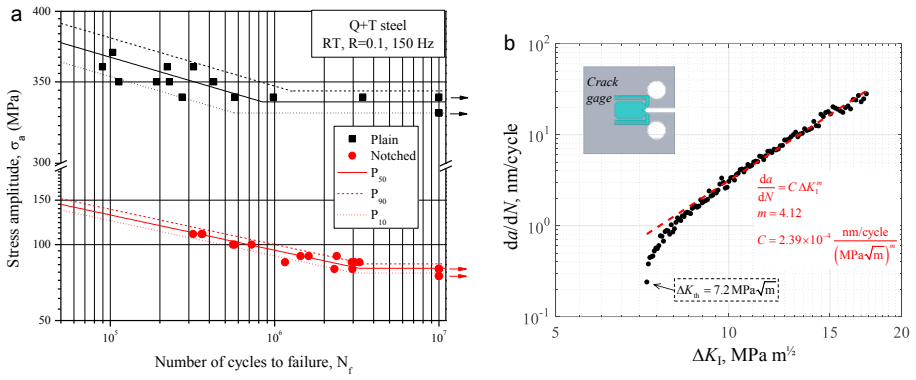

Fig. 7. (a) S-N curves of plain and notched specimens; (b) Paris propagation data and evidence of the threshold value.

Conclusions

- A radiused V-shaped notched specimen was proposed for an optimal critical distance inversion search, mainly to circumvent the threshold experimental determination.
- All the dimensions of this specimen are provided and discussed, in particular the notch root radius which is required to be carefully selected by taking into account the expected critical distance size.
- The determination of the critical distance was performed with a set of simple formulas, based on the self-similitude of the stress solution, thus according to a dimensionless approach. All the required coefficients, derived from a series of accurate finite element simulations, are available in the paper.
- As validation experiment, the critical distance was found with the proposed procedure and then compared to the threshold derived value. This analysis was taken on a common quenched and tempered steel, and very similar lengths resulted for two different load ratios.

Acknowledgements

This work was supported by the University of Pisa under the “PRA – Progetti di Ricerca di Ateneo” (Institutional Research Grants) – Project No. PRA_2016_36.

References

Taylor D., 2007. The Theory of Critical Distances: A New Perspective in Fracture Mechanics, Elsevier, Oxford, UK.
Taylor D., 2008. The theory of critical distances, Engineering Fracture Mechanics 75, 1696–1705.
Benedetti M., Fontanari V., Santus C., Bandini M., 2010. Notch fatigue behaviour of shot peened high-strength aluminium alloys: Experiments and predictions using a critical distance method, International Journal of Fatigue 32, 1600–1611.
Bertini L., Santus C., 2015. Fretting fatigue tests on shrink-fit specimens and investigations into the strength enhancement induced by deep rolling, International Journal of Fatigue 81, 179–190.
Bagni C., Askes H., Susmel L., 2016. Gradient elasticity: a transformative stress analysis tool to design notched components against uniaxial/multiaxial high-cycle fatigue, Fatigue and Fracture of Engineering Materials and Structures 39, 1012–1029.
Benedetti M., Fontanari V., Allahkarami M., Hanan J., Bandini M., 2016. On the combination of the critical distance theory with a multiaxial fatigue criterion for predicting the fatigue strength of notched and plain shot-peened parts, International Journal of Fatigue 93, 133–147.
Taylor D., 2011. Applications of the theory of critical distances in failure analysis, Engineering Failure Analysis 18, 543–549.
Susmel L., Taylor D., 2010. The Theory of Critical Distances as an alternative experimental strategy for the determination of KIc and ΔKth, Engineering Fracture Mechanics 77, 1492–1501.
Hu X., Yang X., Wang J., Shi D., Huang J., 2013. A simple method to analyse the notch sensitivity of specimens in fatigue tests, Fatigue and Fracture of Engineering Materials and Structures 36, 1009–1016.
Atzori B., Lazzarin P., Meneghetti G., 2005. A unified treatment of the mode I fatigue limit of components containing notches or defects, International Journal of Fracture 133, 61–87.
Hills D., Dini D., 2011. Characteristics of the process zone at sharp notch roots, International Journal of Solids and Structures 48, 2177–2183.